Supporting Information

Optimization of a Degradable Polymer-Lipid Nanoparticle for Potent Systemic Delivery of mRNA to the Lung Endothelium and Immune Cells

James C. Kaczmarek[1,2], Kevin J. Kauffman[1,2], Owen S. Fenton[2,3], Kaitlyn Sadtler[2], Asha K. Patel[1,4],Michael W. Heartlein[5], Frank DeRosa[5], Daniel G. Anderson[1,2,6,7,]*

[1]Deparment of Chemical Engineering, [2]David H. Koch Institute for Integrative Cancer Research, [3]Department of Chemistry, [6]Institute for Medical Engineering and Science, and [7]Harvard and MIT Division of Health Science and Technology, Massachusetts Institute of Technology, Cambridge, MA (USA)

[4]Division of Cancer and Stem Cells, School of Medicine, University of Nottingham, Nottingham NG7 2RD (UK)

[5]Translate Bio, Lexington, MA (USA)

*Correspondence Email: dgander@mit.edu

1. Chemical Synthesis and Characterization

Representative Synthesis of A1 Polymer

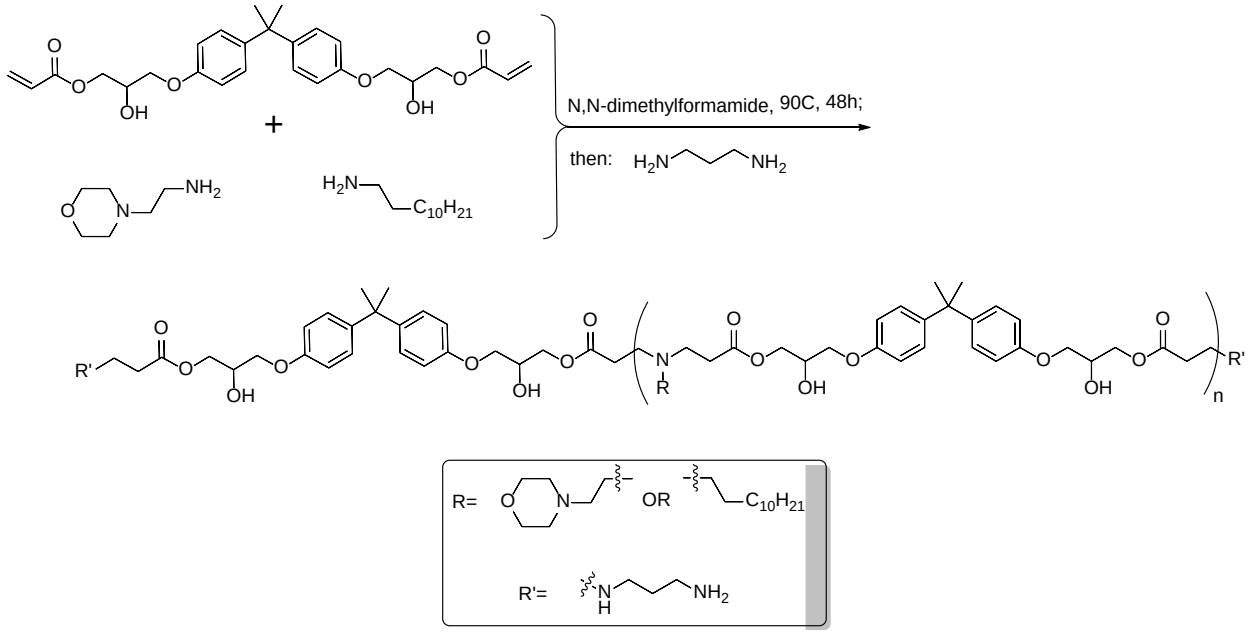

All monomers were pre-dissolved in N,N-dimethylformamide at a concentration of 1 M. To a 5 mL glass scintillation vial were added the bisphenol A glycerolate diacrylate (200 mg, 0.41 mmol, 1.2 equiv), 4-(2-amino methyl) morpholine (22 mg, 0.17 mmol, 0.5 equiv), and dodecyl amine (32 mg, 0.17 mmol, 0.5 equiv). The vial was then sealed, covered in aluminum foil, and heated to 90ºC. After 48 hours, the reaction was cooled to room temperature. The vial was

opened to the air and end-capping amine 1,3-diaminopropane was added in excess (38 mg, 0.51 mmol) and mixed until completely dissolved. The end-capping reaction was allowed to proceed at room temperature for 24 hours, after which the reaction was diluted in diethyl ether at a ratio of 4:1 ether:crude product v/v and vigorously vortexed. The heterogeneous mixture was then centrifuged for 2 minutes at 1250 x *g*. The liquid was then decanted, leaving behind the polymeric solid. The ether wash/centrifugation/decanting process was repeated an additional time, and then the solid was dried under reduced pressure. The resulting polymer was characterized by gel permeation chromatography (GPC), infrared spectroscopy (IR), and ^{1}H nuclear magnetic resonance (NMR). The polymer was stored neat at -20 to -80ºC, with samples taken and dissolved in DMSO at 100 mg/mL as needed.

Other polymer variants were synthesized as above, with molar ratios, end-capping monomer, and alkylamine monomer adjusted as necessary. For library synthesis, diacrylate scale was kept at 200 mg for all reactions, and end-capping monomer was added at a ratio of 1 mmol per 500 mg of diacrylate plus amines.

Instrumentation and Methods

Proton nuclear magnetic resonance (^{1}H and ^{13}C NMR) spectra were recorded with a Varian inverse probe INOVA-500 spectrometer (with a Magnex Scientific superconducting actively-shielded magnet), are reported in parts per million on the δ scale, and are referenced from the residual protium in the NMR solvent (DMSO-d_6: δ2.50)[1] displaying a window range of 9 to -0.5 ppm.

Infrared data (IR) were obtained with a Bruker Alpha FTIR spectrometer. Samples were collected neat on a ZnSe ATR crystal, and spectra are reported as percent absorbance as a function of frequency of absorption (cm^{-1}). Gel Permeation Chromatography of the A1 polymer (GPC) was carried out in tetrahydrofuran (THF) on Styragel columns utilizing a Malvern Viscotek^{TM} TDA 305 triple detection system. Samples were filtered over 0.2 µm PTFE filters before injection using a 1.0 mL/min flow rate. Molecular weights and polydispersities were determined by comparing to a linear polystyrene standard.

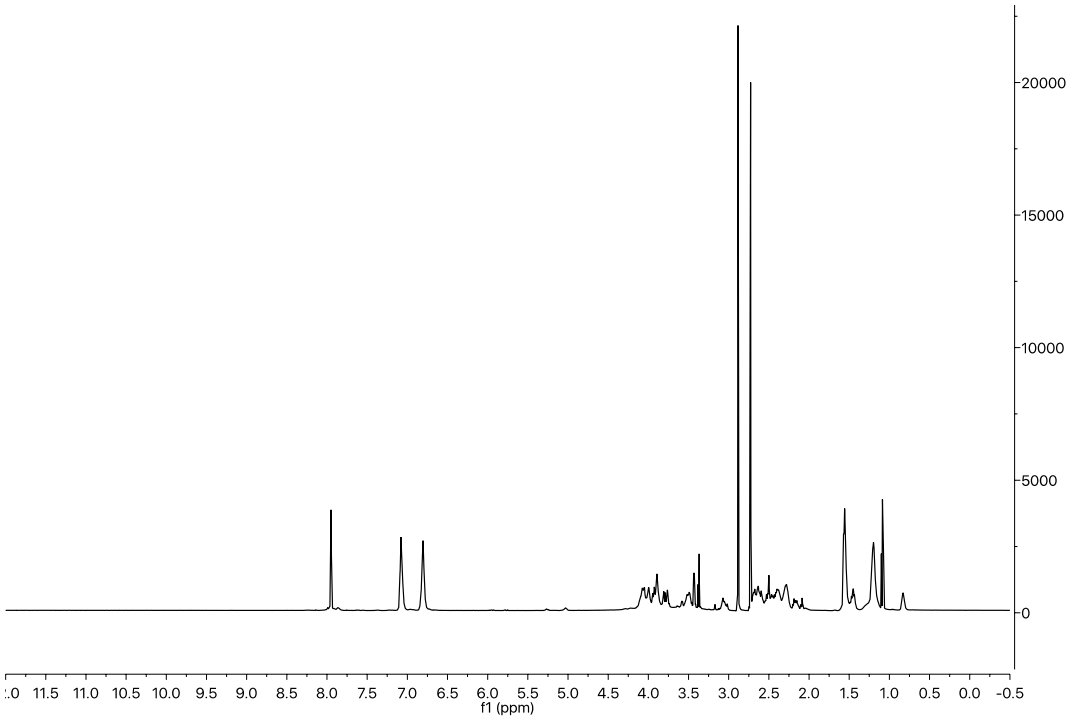
20000
15000
10000
5000
0
11.5 11.0 10.5 10.0 9.5 9.0 8.5 8.0 7.5 7.0 6.5 6.0 5.5 5.0 4.5 4.0 3.5 3.0 2.5 2.0 1.5 1.0 0.5 0.0 -0.5
f1 (ppm)

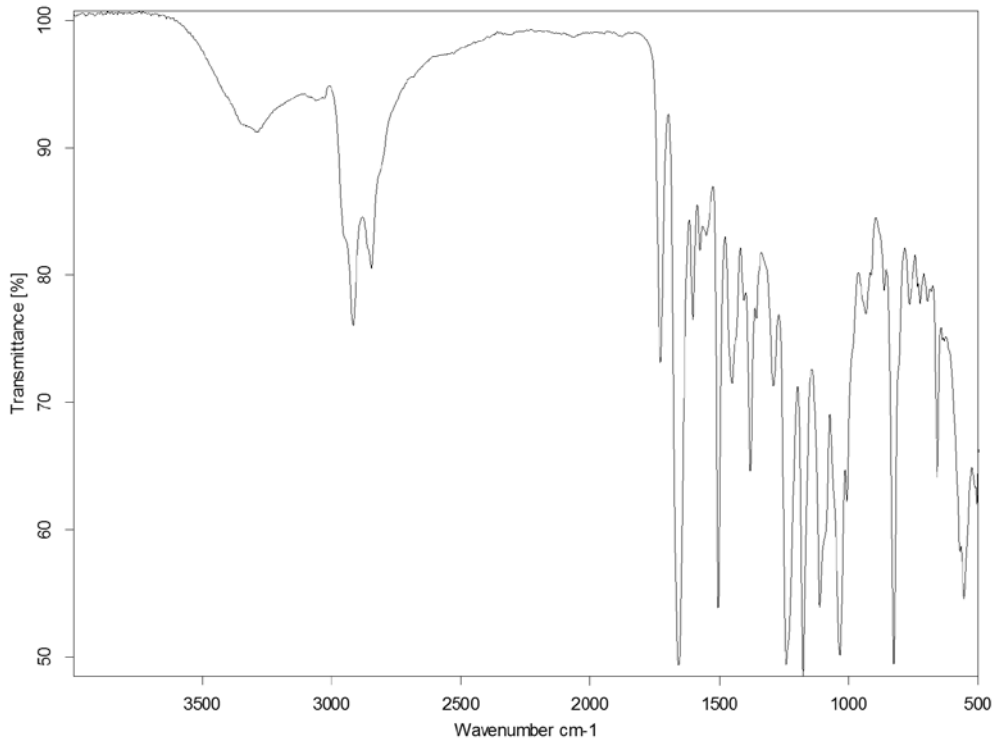
Transmittance [%]
100
90
80
70
60
50
3500
3000
2500
2000
1500
1000
500
Wavenumber cm-1

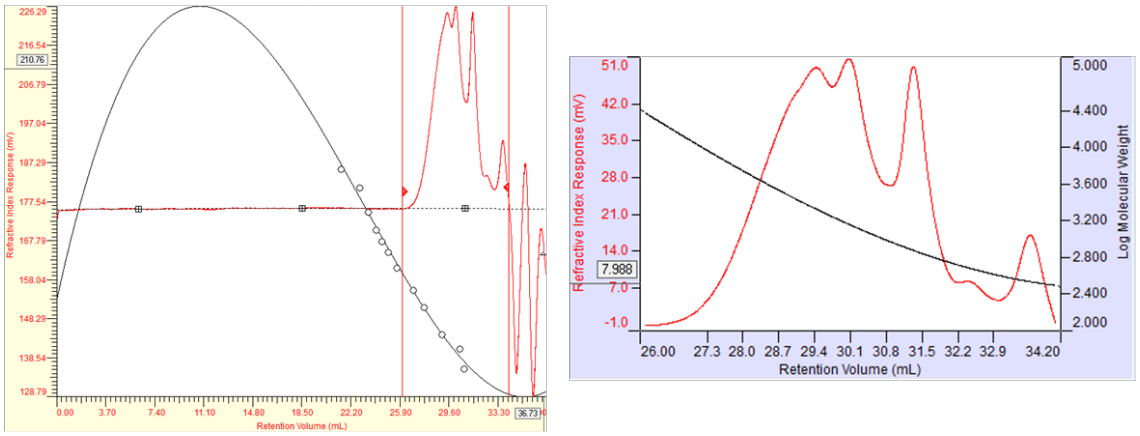

Figure S1: NMR (top left), IR (middle), and GPC (bottom) analysis of poly(bisphenol A glycerolate-*co*-4-(2-amino methyl) morpholine) end capped with 1,3-diaminopropane (A1 polymer).

2. Extended Experimental Methods

Materials

Bisphenol A glycerolate, 4-(2-amino methyl) morpholine, octyl amine (alkylamine C8), dodecyl amine (alkylamine C12), octadecyl amine (alkylamine C18), 1,3-diaminopropane (end cap 1), 1,3-diaminopentane (end cap 3), 2-methyl-1,5-diaminopentane (end cap 4), and cholesterol were purchased from Aldrich (St. Louis, MO). 2,2-dimethyl-1,3-diaminopropane (end cap 2) was purchased from TCI America (Mountain View, CA). (Poly-ethylene oxide)$_4$-bis-amine (end cap 5) was purchased from Molecular Biosciences (Boulder, CO). Heparin sodium salt from porcine intestinal mucosa was obtained from Alfa Aesar (Haverhill, MA). 14:0 PEG1000 PE (C14-PEG1000), 14:0 PEG2000 PE (C14-PEG2000), 14:0 PEG3000 PE (C14-PEG3000), 14:0 PEG5000 PE (C14-PEG5000), 16:0 PEG1000 PE (C16-PEG1000), 16:0 PEG2000 PE (C16-PEG2000), 16:0 PEG3000 PE (C16-PEG3000), 16:0 PEG5000 PE (C16-PEG5000), 18:0 PEG1000 PE (C18-PEG1000), 18:0 PEG2000 PE (C18-PEG2000), 18:0 PEG3000 PE (C18-PEG3000), and 18:0 PEG5000 PE (C18-PEG5000), and 1,2-dioleoyl-sn-glycero-3-phosphoethanolamine (DOPE) were purchased from Avanti Polar Lipids (Alabaster, AL). jetPEI and *in vivo* jetPEI were obtained from VWR (Radnor, PA). Firefly luciferase-encoding mRNA was generously provided by Shire Pharmaceuticals (Lexington, MA). All chemical reagents were used as received with no further purification. NLS-Cre mRNA 100% modified with pseudouridine and 5-methylcytidine, capped with Cap 0, and polyadenylated was purchased from Tri-Link Biotechnologies (San Diego, CA).

mRNA Synthesis

Luciferase-encoding mRNA was a generous gift from Translate Bio, and was synthesized by an *in vitro* transcription from a plasmid DNA template encoding for the firefly luciferase gene. The *in vitro* transcription was followed by the addition of a 5' cap structure (Cap1) using a vaccinia virus-based guanylyl transferase system. FLuc mRNA contained a 5' UTR consisting of a partial sequence of the cytomegalovirus (CMV) immediate early 1 (IE1) gene, a coding region as described below, a 3' UTR consisting of a partial sequence of the human growth hormone (hGH) gene, and a 3' polyA tail (~300 nt).

AUGGAAGAUGCCAAAAACAUUAAGAAGGGCCCAGCGCCAUUCUACCCACUCGAAGACGG
GACCGCCGGCGAGCAGCUGCACAAAGCCAUGAAGCGCUACGCCCUGGUGCCCGGCACC
AUCGCCUUUACCGACGCACAUAUCGAGGUGGACAUUACCUACGCCGAGUACUUCGAGAU
GAGCGUUCGGCUGGCAGAAGCUAUGAAGCGCUAUGGGCUGAAUACAAACCAUCGGAUC
GUGGUGUGCAGCGAGAAUAGCUUGCAGUUCUUCAUGCCCGUGUUGGGUGCCCUGUUCA
UCGGUGUGGCUGUGGCCCCAGCUAACGACAUCUACAACGAGCGCGAGCUGCUGAACAG
CAUGGGCAUCAGCCAGCCCACCGUCGUAUUCGUGAGCAAGAAAGGGCUGCAAAAGAUC
CUCAACGUGCAAAAGAAGCUACCGAUCAUACAAAAGAUCAUCAUCAUGGAUAGCAAGACC
GACUACCAGGGCUUCCAAAGCAUGUACACCUUCGUGACUUCCCAUUUGCCACCCGGCU
UCAACGAGUACGACUUCGUGCCCGAGAGCUUCGACCGGGACAAAACCAUCGCCCUGAU
CAUGAACAGUAGUGGCAGUACCGGAUUGCCCAAGGGCGUAGCCCUACCGCACCGCACC
GCUUGUGUCCGAUUCAGUCAUGCCCGCGACCCCAUCUUCGGCAACCAGAUCAUCCCCG
ACACCGCUAUCCUCAGCGUGGUGCCAUUUCACCACGGCUUCGGCAUGUUCACCACGCU
GGGCUACUUGAUCUGCGGCUUUCGGGUCGUGCUCAUGUACCGCUUCGAGGAGGAGCU
AUUCUUGCGCAGCUUGCAAGACUAUAAGAUUCAAUCUGCCCUGCUGGUGCCCACACUAU
UUAGCUUCUUCGCUAAGAGCACUCUCAUCGACAAGUACGACCUAAGCAACUUGCACGAG
AUCGCCAGCGGCGGGGGCGCCGCUCAGCAAGGAGGUAGGUGAGGCCGUGGCCAAACGC
UUCCACCUACCAGGCAUCCGCCAGGGCUACGGCCUGACAGAAACAACCAGCGCCAUUCU
GAUCACCCCCGAAGGGGACGACAAGCCUGGCGCAGUAGGCAAGGUGGUGCCCUUCUUC
GAGGCUAAGGUGGUGGACUUGGACACCGGUAAGACACUGGGUGUGAACCAGCGCGGCG
AGCUGUGCGUCCGUGGCCCCAUGAUCAUGAGCGGCUACGUUAACAACCCCGAGGCUAC
AAACGCUCUCAUCGACAAGGACGGCUGGCUGCACAGCGGCGACAUCGCCUACUGGGAC
GAGGACGAGCACUUCUUCAUCGUGGACCGGCUGAAGAGCCUGAUCAAAUACAAGGGCU
ACCAGGUAGCCCCAGCCGAACUGGAGAGCAUCCUGCUGCAACACCCCAACAUCUUCGAC
GCCGGGGUCGCCGGCCUGCCCGACGACGAUGCCGGCGAGCUGCCCGCCGCAGUCGUC
GUGCUGGAACACGGUAAAACCAUGACCGAGAAGGAGAUCGUGGACUAUGUGGCCAGCC
AGGUUACAACCGCCAAGAAGCUGCGCGGUGGUGUUGUGUUCGUGGACGAGGUGCCUAA
AGGACUGACCGGCAAGUUGGACGCCCGCAAGAUCCGCGAGAUUCUCAUUAAGGCCAAG
AAGGGCGGCAAGAUCGCCGUGUAA

Scrambled-sequence mRNA was transcribed from a DNA plasmid containing a T7 promoter upstream of the coding region. The plasmid was linearized using restriction enzyme Xbal (New England Biolabs, Ipswich, MA) and transcribed using the HiScribe T7 RNA Synthesis Kit (New England Biolabs). mRNA was capped with the Vaccinia Capping System (New England Biolabs), and the cap was modified to Cap1 using mRNA cap 2'-*O*-Methyltransferase (New England Biolabs). A polyA (estimated to be approximately 100 nucleotides long) tail was added to the RNA using a Poly(A) Polymerase Kit (New England Biolabs). mRNA was purified after the transcription and tailing steps using MEGAClear RNA purification columns (Life Technologies, Beverly, MA). RNA concentration was determined using a NanoDrop 1000 (Thermo Scientific, Cambridge, MA). The mRNA sequence used is given below:

AUGGUUCGAGGGUGAACGAAGCGACUGUCUCGGCGGUUCCCCCUAGCCACGGGUGAGA
GAGUUGACGCCGCGAGUCGCGAGUGGACAGUGCGGCUGCGGCUCGGACGUUGACCGA
CAGUGAGAGGACCGGCACACAGAGCCCACACCUCCCGUCAGCCAUUCGCUACCUUGUG
AGGCGUUGGGACUCUUUUCCGGUGGGGAUCCGCCGAUCACGACGCCUUGCUAGACCG
GGGGCUGUGAAUCCACCCAAGAUCUUUAUCUGGCUGGGUGGCGACUGCGCGCUUGACG
CGCGACCGACCCCGAGCAAAGUCAUAACAUAGUGGAGCCUGGUUGUGUGGCUGUCGAA
UACCCCUUUGGCGUGUUCAGGACGAAGGGGCGUCAUUUGUCACCGGUGAUCACCAUCG
UGCCAGACCGAGCGCACACUACACGAGCUGCUUAGACCGCAUAUCAUACGGAAGGGUC
UCCCUACUUCCCACGACUCCUUUUGACAGUUCUCACAUCCUCGUGAGUCAGCGCCCGC

GAGCCUAUUUUACGUGGCACUAGGCCUCCGACCCAGUCGCCUCACCACACGAAACCCU
GUA

Nanoparticle Synthesis

mRNA was diluted in 25 mM sodium acetate (NaOAc) buffer while the appropriate amounts of polymer and PEG-lipid were co-dissolved in 200 proof ethanol. For particles synthesized by hand mixing, the aqueous:ethanol phase ratio was 1:1 v/v, and particle formation was performed by adding the ethanol phase to the aqueous phase and mixing vigorously. Nanoparticles formulated via microfluidic device[2] were synthesized at a 3:1 v/v ratio of mRNA phase to the polymer phase. For particles formulated with only PEG-lipid, little difference in efficacy was apparent between the pipette-mixing and microfluidic-mixing strategies (Fig. S9). Nanoparticles were then dialyzed against PBS in a 20000 MWCO cassette at 4°C for 2-3 hours. jetPEI nanoparticles were made according to supplier protocol. Briefly, jetPEI and RNA were diluted in equal volumes of the provided buffer in order to yield the desired N/P. The jetPEI phase was added to the RNA phase and was mixed by vortexing, and the resulting nanoparticles were incubated at room temperature for 15 minutes prior to use. All particles were used no earlier than 15 minutes and no later than 4 hours following synthesis.

Nanoparticle Characterization

The mRNA concentration in dialyzed particles was determined via a modified Quant-iT RiboGreen RNA assay (Thermo Fisher). A nanoparticle dilution of ~1 ng μL^{-1} mRNA was made in TE buffer (pH 8.5) and mRNA standards were made ranging from 2 ng μL^{-1} to 0.125 ng μL^{-1}. 50 µL of each solution was added to separate wells in a 96-well black polystyrene plate. To each well was added either 50 µL of 10 mg/mL heparin in TE buffer, which disrupted the electrostatic forces binding the polymer and mRNA to allow for accurate quantification of nanoparticle mRNA content, or 50 µL of un-supplemented TE buffer. The plate was incubated at 37ºC for 15 minutes with shaking at 350 rpm. Following the incubation, the diluted RiboGreen reagent was added (100 µL per well), and the plate was incubated as before for 3 minutes. RiboGreen fluorescence was measured according to the supplied protocol using a Tecan plate reader, and the mRNA standard was used to determine nanoparticle mRNA concentration. It should be noted that two separate standards were made: one with and one without 10 mg/mL heparin. The particles in heparin were used to determine mRNA concentration, and encapsulation efficiency was determined via the following equation:

$$EE = \left(1 - \frac{Conc_{TE}}{Conc_{Hep}}\right)$$

where $Conc_{TE}$ and $Conc_{Hep}$ are the concentration readings for particles without and with heparin, respectively. Nanoparticle size was measured via dynamic light scattering via a standard (Nano ZS, Malvern) or high-throughput (Dyna Pro Plate Reader, Wyatt) system. For size measurement, particles were diluted in PBS at a 1:16 v/v ratio and an intensity average measurement was reported for particle size.

In vitro transfections

HeLa cells (ATCC) were cultured in Dulbecco's Modified Eagle Medium (Invitrogen) supplemented with 10% v/v heat inactivated fetal bovine serum (Invitrogen) and 1% v/v Penicillin Streptomycin (Invitrogen). 24 hours before transfection, cells were seeded onto a 96-

well polystyrene tissue culture plate (20,000 cells per well, 100 µL media containing serum and antibiotic per well). In a typical example, mRNA-loaded nanoparticles were diluted to 5 ng μL^{-1} in buffer and mixed with media such that the volume ratio of nanoparticle solution to media was 1:9. The media in the plate was aspirated, and the nanoparticle-containing media was added to the wells, in this case at a final concentration of 50 ng mRNA per well. Note that for all doses reported (e.g. mRNA/uL, mRNA/well, or mRNA/kg of animal), the mass of mRNA refers to the mass of mRNA complexed with the polymer nanoparticles. 24 hours following transfection, cell viability was assayed using a MultiTox-Fluor Multiplex Cytotoxicity Assay (Promega) and cellular luminescence was quantified using Bright-Glo Assay kits (Promega), both of which were measured using a Tecan plate reader. Cellular luminescence was normalized to live cell fluorescent signal. No wash step was used following particle transfection.

Animal Studies

All animal experiments were approved by the M.I.T. Institutional Animal Care and Use Committee and were consistent with local, state, and federal regulations as applicable. Female C57BL/6 mice (Charles River Laboratories, 18-22g) were intravenously injected with nanoparticles via the tail vein. For luciferase imaging experiments, mice were injected intraperitoneally with 130 µL of 30 mg mL^{-1} D-luciferin (PerkinElmer) in PBS 24 hours after injection. 10 minutes following luciferin injection, mice were sacrificed via CO_2 asphyxiation. Six organs were collected (pancreas, spleen, kidneys, liver, lungs, and heart) and imaged for luminescence using an IVIS imaging apparatus (PerkinElmer) with the luminescence being quantified using Living Image Software (PerkinElmer). For Cre mRNA experiments, female B6.Cg-Gt(ROSA)26Sortm14(CAG-tdTomato)Hze/J (Ai14) mice (Jackson Laboratories, 18-22g) were intravenously injected with nanoparticles via the tail vein. 48 hours post-injection, mice were sacrificed via CO_2 asphyxiation and their lungs were harvested for single cell processing. Saline-treated wild type C57BL/6 mice were used as controls for experiments probing gross immune and endothelial expression. To account for differences in immune cell populations following nanoparticle treatment, Ai14 mice treated with A1-L3 PBAEs carrying a scramble mRNA sequence were used as controls for experiments identifying transfected immune cell subpopulations.

Liver Enzyme Level Testing

Alanine transaminase (ALT) and aspartate transaminase (AST) activity kits were purchased from Sigma Aldrich (St. Louis, MO). Whole blood was obtained from mice via tail vein bleed 24 hours following nanoparticle dosing in serum collection tubes (Sarstedt). The tubes were then centrifuged according to manufacturer instruction to enable plasma collection. Plasma was then diluted in sample buffer from activity kits, and the colorimetric assay was run per manufacturer instruction. ALT and AST levels were normalized to PBS-treated mice.

Flow Cytometry

Lungs were digested in a mixture of collagenase I (450 U), collagenase XI (125 U), and DNase I (2 U) in 1 mL PBS at 37ºC with constant agitation for 1 hr. The digest was passed through a 70 µm filter, followed by centrifugation. The supernatant was then removed, and cells were treated with red blood cell lysis buffer for 5 min at 4ºC. The lysis buffer was then quenched with PBS, and the cells were then centrifuged again with the supernatant removed afterwards. The cells were then suspended in flow buffer (PBS containing 0.5% BSA and 2 mM EDTA) and passed through a 40 µm filter. Cells were incubated with viability dye (eBioscience Fixable Viability Dye eFluor 780, Invitrogen) at a 1:1000 dilution at 4°C for 30 minutes, followed by a wash with flow

buffer. Surface staining of cells with fluorescent antibodies was then performed using the antibodies and dilutions listed in Table S7 at 4ºC in flow buffer for 30-60 min. Following surface staining, cells were washed twice with and then re-suspended in flow buffer for analysis.

Gating strategies for cell population identification can be found in Figures S14-16, and antibodies and dilutions can be found in Table S7. Data was collected using a BD LSR II or Fortessa cytometer (BD Biosciences) and analyzed with FlowJo software (Ashland, OR).

Statistics

Data were expressed as mean ± SD for groups of at least three replicates, or as individual values with the mean indicated. All statistical analyses for design of experiments modeling were performed using JMP Pro 12 software. Other statistical analysis (e.g. of graphical data) were performed using an unpaired, two-tailed student's t test in Graphpad Prism 7.

3. Experimental Design Methodology

In general, experimental design applies statistical methodologies in order to reduce a design space while maintaining enough information to determine variables (or combinations of variables) which have a significant effect on an outcome. In other words, experimental design strategically "picks" a limited number of test conditions from a full factorial set that will maximize (based on the desired resolution) the conclusions that can be drawn about independent variable effects on dependent variables. There are many algorithms that can be used determine which conditions will be chosen from the set,[3] which leads to a variety of ways in which experimental design can be executed and a variety of interaction levels between dependent variables that can be accurately assessed.

The majority of this section will be focused on the specifics of design choices made for this particular study. For a more general explanation of applying experimental design to nanoparticle formulation, the reader is directed to the supplementary information of the following paper.[4]

Synthesis Screen

All experimental design was done using JMP Pro 12 software. The variables and their levels for the synthesis screen are shown in Table S1. For the synthesis screen, we were concerned mainly with first order effects, and as such applied the default JMP algorithm to determine conditions for a fractional factorial screen for main effects. We wanted to test all continuous variables at three levels (in order to observe any nonlinear effects) along with 5 levels of the categorical end-capping variable (corresponding to 5 different end caps tested), and we chose to test 30 conditions (Table S2). In all cases, due to the range of values obtained, the $\log_{10}$ of luciferase expression was used to build the statistical model in order to keep samples with very high (or very low) efficacy from skewing the results.

Table S1: Parameter range for synthesis screen.

Parameter	Range	"A1" PBAE
Diacrylate:Total Amine Ratio	1:1 – 1.2:1	1.2:1
Alkylamine:Amine Ratio	1:9 – 1:1	1:1
Hydrophobic Amine Length	8 - 18	12
End Cap	5 monomers	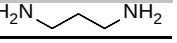

Table S2 : Conditions for synthesis screen (polymer structure included for clarity).

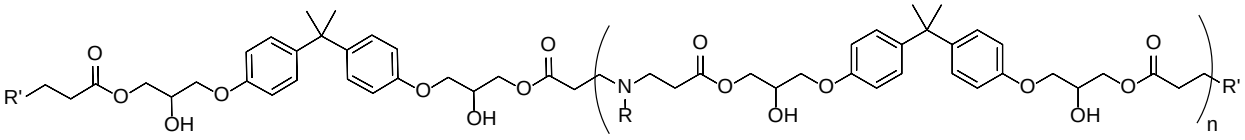

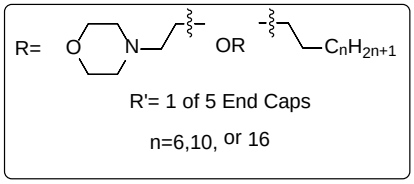

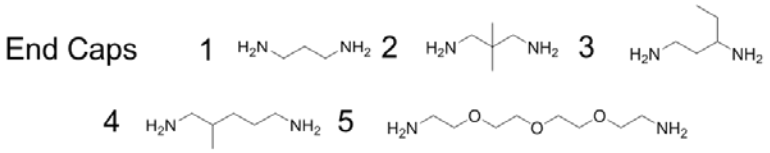

Polymer ID	Diacrylate:Amine Ratio	Alkylamine mol%	Alkylamine Length	End Cap ID
A1	1.2	50	12	1
A2	1.1	50	8	3
A3	1	50	18	2
A4	1.1	10	12	5
A5	1.1	50	8	1
A6	1	50	12	3
A7	1.1	50	18	5
A8	1	10	12	1
A9	1.1	30	18	4
A10	1.2	30	18	1
A11	1.1	10	18	1
A12	1.2	30	8	2
A13	1	50	12	2
A14	1.1	30	12	4
A15	1	50	12	4
A16	1.1	30	12	3
A17	1	10	8	4
A18	1.2	10	12	5
A19	1.2	10	8	4
A20	1.2	50	18	4
A21	1.2	50	8	5
A22	1.2	10	8	3
A23	1	30	8	1
A24	1	10	18	3
A25	1.1	10	18	2
A26	1.1	10	8	2
A27	1	30	18	5
A28	1	30	8	5
A29	1.2	30	12	2
A30	1.2	30	18	3

Figure S2a displays the parameter estimates (i.e. the probability a parameter has a significant effect) for the statistical model (based on a linear least squares regression) before eliminating insignificant variables and Fig. S2b displays the same table after elimination of insignificant variables. As can be seen, only the end capping variable, specifically only the 103 monomer, remained, meaning it is the only variable that exhibited a statistically significant effect on the model. As stated in the text, since previous large-scale end capping screens already identified the 5 end caps used herein as the most potent for PBAE nucleic acid delivery, further optimization was not deemed necessary.

a

Parameter Estimates

Term	Estimate	Std Error	t Ratio	Prob>|t|
Intercept	1.6676106	0.132411	12.59	<.0001*
Diacrylate:Amine Ratio(1,1.2)	0.04513	0.161955	0.28	0.7831
Alkylamine mol%(10,50)	0.0050428	0.161955	0.03	0.9754
Hydrophobic Amine Length(8,18)	0.0203536	0.160812	0.13	0.9004
End Cap[103]	0.5925202	0.263952	2.24	0.0352*
End Cap[116]	-0.49148	0.263952	-1.86	0.0760
End Cap[117]	-0.467752	0.263952	-1.77	0.0902
End Cap[118]	0.2632823	0.263952	1.00	0.3294

b

Parameter Estimates

Term	Estimate	Std Error	t Ratio	Prob>|t|
Intercept	1.6662537	0.124062	13.43	<.0001*
End Cap[103]	0.5925202	0.248124	2.39	0.0248*
End Cap[116]	-0.49148	0.248124	-1.98	0.0587
End Cap[117]	-0.467752	0.248124	-1.89	0.0711
End Cap[118]	0.2632823	0.248124	1.06	0.2988

c

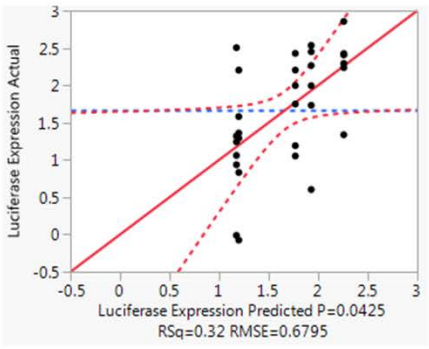

d

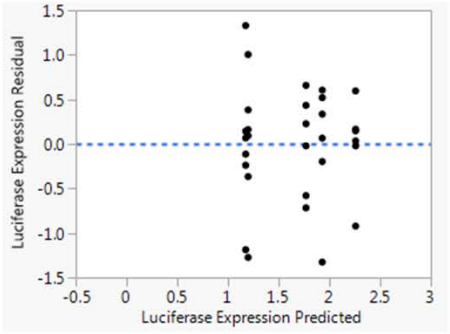

Figure S2. Model results before (a) and after (b) non-significant effects were removed. Note that the 122 end cap is not included because all of the parameter estimates of the discrete attributes under the "end cap" variable will sum to 0 (that is, only 4/5 attributes within the "end cap" variable are independent). The ultimate model prediction versus the actual results is shown in (c), with its residuals given in (d).

Importantly, a distinction must be made between variables which are statistically significant as main variables to the model and variables which exhibit an observable effect on the system. Clearly, the end cap was not the only variable to affect particle efficacy, as not all polymers end capped with a given monomer had the same efficacy. The other variables simply were not statistically significant in and of themselves, meaning: 1) The variables were only significant at a higher order, which cannot accurately be estimated by a model designed to screen for main effects, or, perhaps less likely, 2) The effect of the variable exhibited no definitive unidirectional trend, which is possible for levels >2.

Definitive Formulation Screen

As is stated in the main text, a definitive screen was chosen for the first formulation screen in an attempt to narrow the large design space that came with limited research into hydrophobic formulations with PBAE terpolymer nanoparticles. Table S3 displays the variable ranges chosen, based off of values commonly used for lipid nanoparticles.[4] Model analysis, as done previously, revealed that DOPE mol% was the only statistically significant variable (Fig. S3). This, and the formulation parameters for the D2 formulation which outperformed the original, was taken into account in designing the next screen.

Table S3: Parameter ranges for synthesis screens.

Parameter	Definitive Screen Range	Partial Factorial Screen Range	PEG-lipid Screen Range	"L3" Formulation
N/P	25 - 100	50 - 75	X	50
PEG-lipid mol%	1 - 10	2 - 9	1 - 7	5
PEG-lipid PEG MW	1000 - 5000	1000 - 3000	X	2000
PEG-lipid C length	12 - 18	X	X	18
DOPE mol %	0 - 20	20 - 50	X	20
Cholesterol mol%	0 - 50	X	X	0

Table S4: Conditions for definitive formulation screen.

Formulation ID	N/P	PEG-lipid C Length	PEG-lipid PEG MW	PEG-lipid mol%	Cholesterol mol%	DOPE mol %
D1	62.5	14	1000	1	0	0
D2	100	18	1000	5.5	0	20
D3	100	14	5000	10	0	10
D4	25	14	1000	10	25	20
D5	25	16	5000	1	0	20
D6	100	18	5000	1	25	0
D7	25	14	5000	5.5	50	0
D8	62.5	16	3000	5.5	25	10
D9	62.5	18	5000	10	50	20
D10	100	16	1000	10	50	0
D11	25	18	3000	10	0	0
D12	25	18	1000	1	50	10
D13	100	14	3000	1	50	20

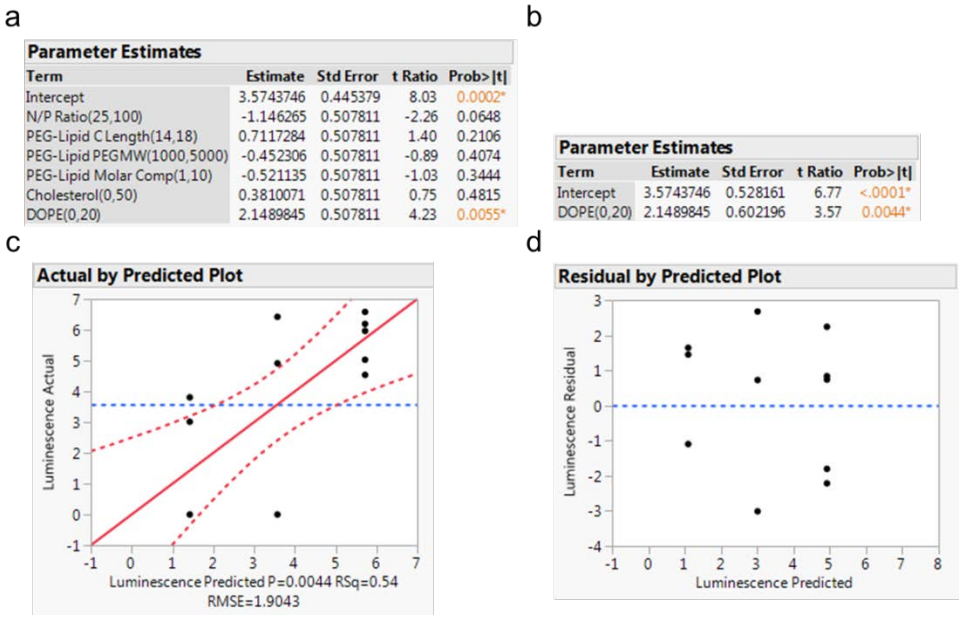

Figure S3. Definitive screen model results before (a) and after (b) non-significant effects were removed. The ultimate model prediction versus the actual results is shown in (c), with its residuals given in (d).

Partial Factorial Formulation Screen

As with the synthesis screen, we were next interested in identifying key main effects from remaining variables using a partial factorial screen. We shifted the parameter space (Table S5) from the definitive screen according to the following logic:

- Cholesterol was eliminated as it had by far the least influence on the definitive screen model, and the D2 formulation had no cholesterol (Fig. S3a)
- DOPE mol% had its lowest value adjusted to 20 mol% since it demonstrated a significant positive effect on efficacy in the previous model
- PEG-lipid mol% had its range decreased to center on the D2 formulation value of 5.5 mol%
- N/P range was moved upward to account for the N/P of 100 in the D2 formulation, but was lowered from the max of 100 due to concerns regarding particle toxicity and stability
- PEG-lipid PEG MW range was adjusted closer to the value in the D2 formulation; the range was not centered on D2 as pilot studies revealed issues with particle stability with PEG MWs less than 1000
- PEG-lipid lipid length was eliminated in order to limit the variable number (and therefore maximize the information available from a given number of runs); this variable was chosen because 2 other PEG-lipid variables were already included. PEG-lipids with 18-carbon tails were chosen for subsequent screens based on the D2 formulation.

Table S5 shows the formulations generated using the JMP software to develop a partial factorial screen consisting of 18 conditions.

Table S5: Conditions for partial factorial formulation screen.

Formulation ID	N/P	PEG-lipid MW	PEG-lipid mol%	DOPE mol%
P1	50	2000	9	35
P2	75	1000	9	50
P3	75	1000	5.5	35
P4	75	3000	9	20
P5	75	2000	2	50
P6	50	1000	2	20
P7	50	1000	5.5	50
P8	50	3000	2	20
P9	62.5	1000	9	20
P10	75	2000	5.5	20
P11	50	2000	9	35
P12	62.5	3000	9	50
P13	62.5	2000	2	50
P14	62.5	2000	5.5	20
P15	50	3000	5.5	50
P16	75	3000	2	35
P17	62.5	1000	2	35
P18	62.5	3000	5.5	35

Given the lack of lung specificity of these formulations (Figure 3, main text), we wanted to build two separate models for this screen: one for lung efficacy (Fig. S4) and one for spleen efficacy (Fig S5). As can be seen, both have a strong negative correlation with PEG-lipid mol%. As discussed in the main text, this also prompted us to investigate the particle diameter. Thus, a third model was built, using particle diameter as the dependent variable of interest (Fig. S6).

a

Parameter Estimates

Term	Estimate	Std Error	t Ratio	Prob>|t|
Intercept	5.0866607	0.15339	33.16	<.0001*
N/P(50,75)	0.2259569	0.187864	1.20	0.2505
DOPE mol%(20,50)	-0.943714	0.187864	-5.02	0.0002*
PEG-Lipid mol%(2,9)	-0.97986	0.187864	-5.22	0.0002*
PEG MW(1000,3000)	-0.211545	0.187864	-1.13	0.2805

b

Parameter Estimates

Term	Estimate	Std Error	t Ratio	Prob>|t|
Intercept	5.0866607	0.157001	32.40	<.0001*
DOPE mol%(20,50)	-0.943714	0.192287	-4.91	0.0002*
PEG-Lipid mol%(2,9)	-0.97986	0.192287	-5.10	0.0001*

c

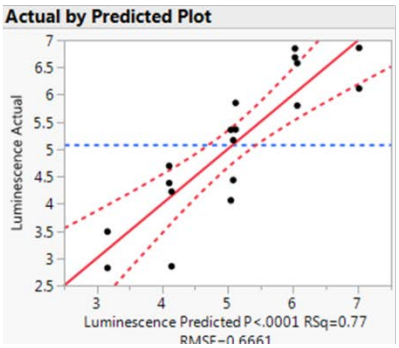

d

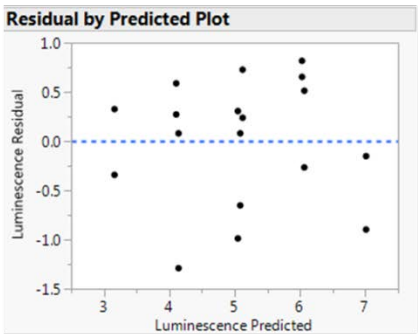

Figure S4. Partial factorial formulation screen lung efficacy model results before (a) and after (b) non-significant effects were removed. The ultimate model prediction versus the actual results is shown in (c), with its residuals given in (d).

a

Parameter Estimates

Term	Estimate	Std Error	t Ratio	Prob>|t|
Intercept	5.6561734	0.140733	40.19	<.0001*
N/P(50,75)	0.2745739	0.172362	1.59	0.1352
DOPE mol%(20,50)	-0.635963	0.172362	-3.69	0.0027*
PEG-Lipid mol%(2,9)	-0.935169	0.172362	-5.43	0.0001*
PEG MW(1000,3000)	-0.529996	0.172362	-3.07	0.0089*

b

Parameter Estimates

Term	Estimate	Std Error	t Ratio	Prob>|t|
Intercept	5.6561734	0.14826	38.15	<.0001*
DOPE mol%(20,50)	-0.635963	0.181581	-3.50	0.0035*
PEG-Lipid mol%(2,9)	-0.935169	0.181581	-5.15	0.0001*
PEG MW(1000,3000)	-0.529996	0.181581	-2.92	0.0112*

c

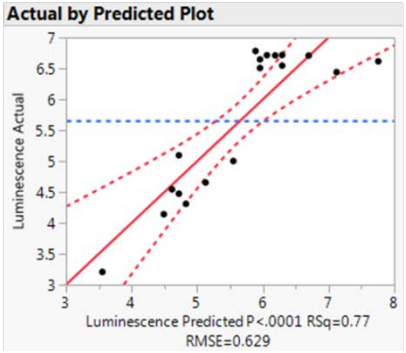

d

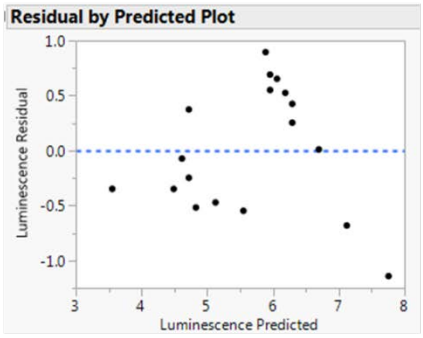

Figure S5. Partial factorial formulation screen spleen efficacy model results before (a) and after (b) non-significant effects were removed. The ultimate model prediction versus the actual results is shown in (c), with its residuals given in (d).

a

Parameter Estimates

Term	Estimate	Std Error	t Ratio	Prob>|t|
Intercept	5.0866607	0.15339	33.16	<.0001*
N/P(50,75)	0.2259569	0.187864	1.20	0.2505
DOPE mol%(20,50)	-0.943714	0.187864	-5.02	0.0002*
PEG-Lipid mol%(2,9)	-0.97986	0.187864	-5.22	0.0002*
PEG MW(1000,3000)	-0.211545	0.187864	-1.13	0.2805

b

Parameter Estimates

Term	Estimate	Std Error	t Ratio	Prob>|t|
Intercept	5.0866607	0.157001	32.40	<.0001*
DOPE mol%(20,50)	-0.943714	0.192287	-4.91	0.0002*
PEG-Lipid mol%(2,9)	-0.97986	0.192287	-5.10	0.0001*

c

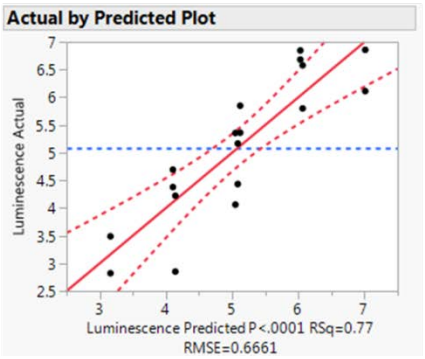

d

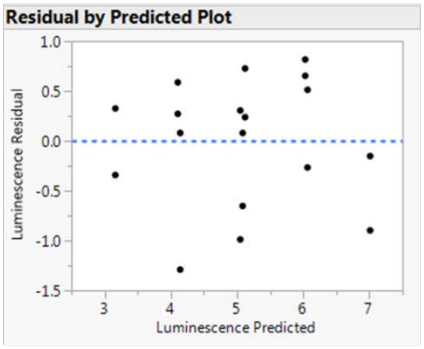

Figure S6. Partial factorial formulation screen nanoparticle diameter model results before (a) and after (b) non-significant effects were removed. The ultimate model prediction versus the actual results is shown in (c), with its residuals given in (d).

As we hypothesized, PEG-lipid mol% had a significant effect on particle diameter, just as it did on spleen and lung efficacy. We therefore wanted to investigate any correlation between particle size and efficacy, both in the lungs and spleen. As can be seen in Figure S7, the diameters clustered into a "large" (>300 nm diameter) and "small" (<100 nm diameter) region, which corresponded with consistent spleen efficacy and low overall efficacy, respectively. Thus, as stated in the main text, we next hypothesized that particles within the "middle" region with respect to diameter may result in greater lung specificity.

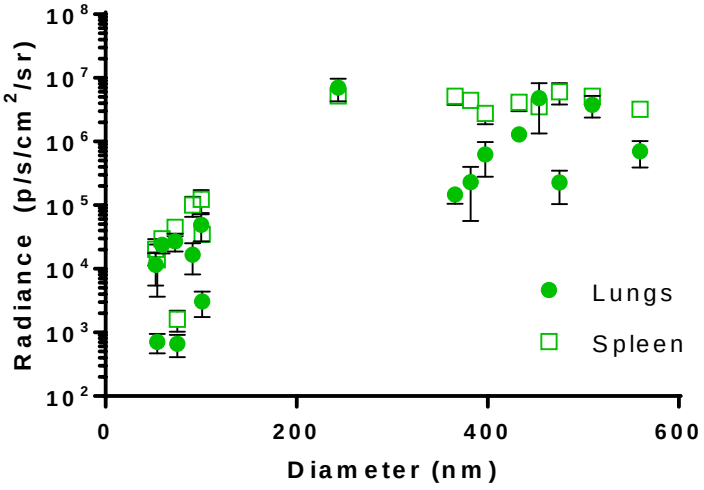

Figure S7. Correlation between diameter and luciferase signal for the partial factorial formulation screen. The two clusters of diameter, <100 nm and >300 nm, correspond with low efficacy and consistently high spleen efficacy, respectively (n = 3).

PEG-lipid Screen

For this final screen, our goal was to vary the PEG-lipid content of the nanoparticles in order to obtain particles within the range of interest. As for setting the other parameters varied in the previous screen, the logic was as follows:

- N/P was not a significant variable in either the lungs or the spleen, and was therefore set to the bottom of the tested range (50) to minimize toxicity
- PEG MW was set to 2000, as the only formulation within the ~100 - ~300 nm range from the previous screen, P14, had a PEG MW of 2000
- DOPE mol% was set to 20; the definitive screen showed a strong positive correlation between DOPE mol% and efficacy (0-20), while the partial factorial screen (0-50 mol%) showed a strong negative correlation between the two, suggesting 20 mol% to be the near optimum

Table S6 shows the conditions used for this screen, based on PEG-lipid amounts that yielded particle diameters within the range of interest (Fig. S8). As shown in Figure 3 within the main text, these particles were, as hypothesized, more lung specific, and both the specificity and efficacy were dependent on PEG-lipid incorporation.

Table S6: Conditions for the PEG-lipid screen.

Formulation ID	PEG-lipid mol%
L1	1
L2	1.5
L3	5
L4	6
L5	7

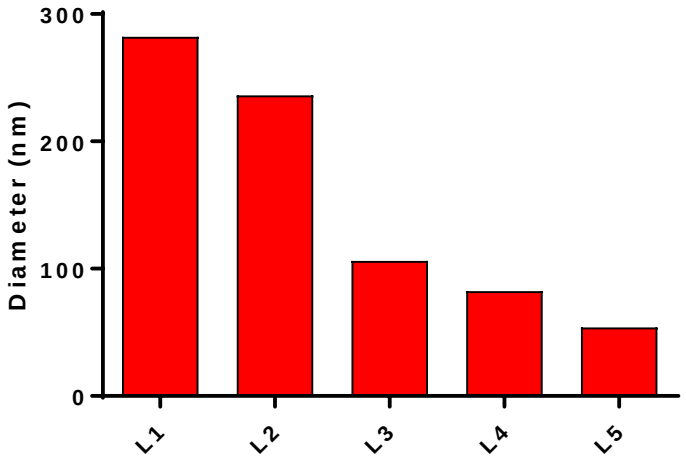

Figure S8. Diameters of particles from the PEG-lipid screen.

4. Additional Data

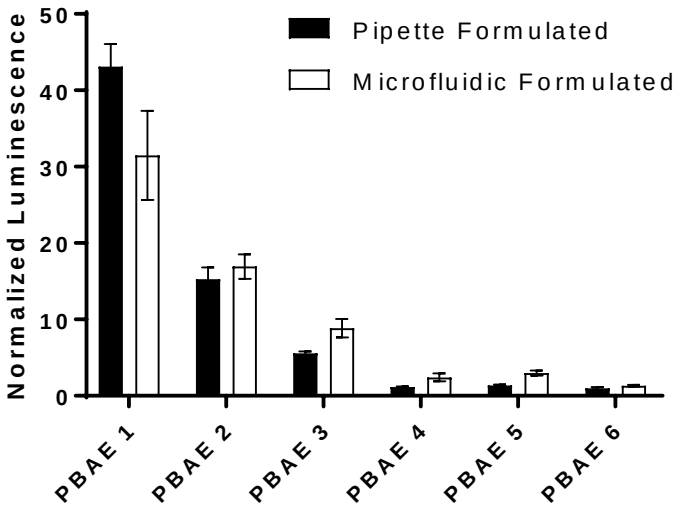

Figure S9. Pilot study with various PBAEs (used in previous studies[5]) delivering luciferase-coding mRNA in HeLa cells demonstrating little difference between microfluidic formulated and pipette formulated particles when PEG-lipid (7 mol%) is the only additional excipient added (n = 4).

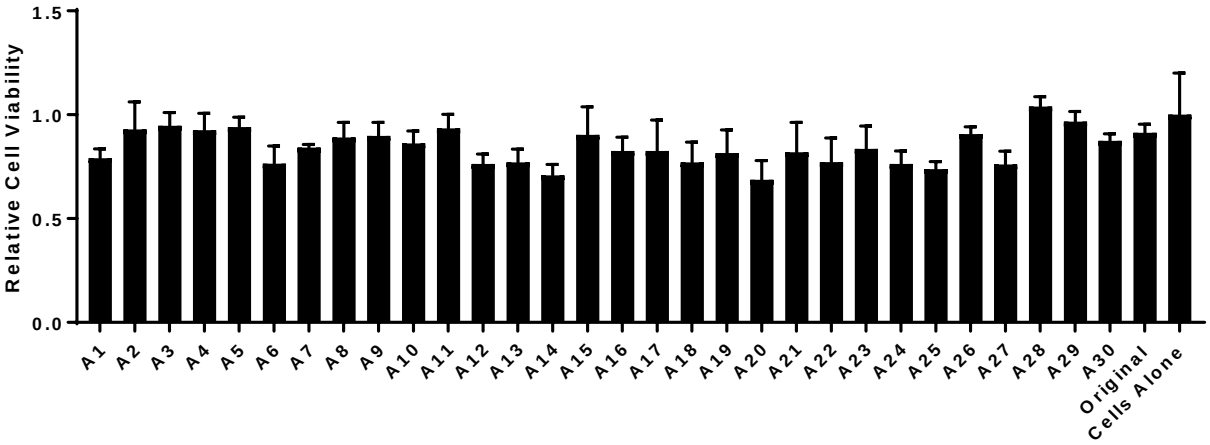

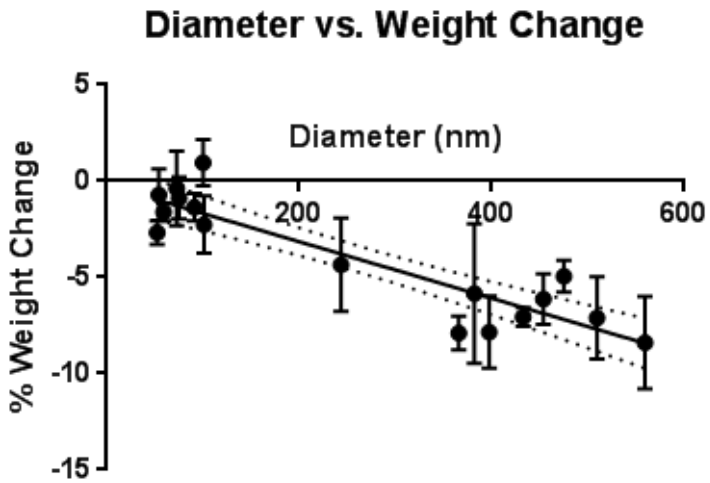

Figure S10. Additional toxicity data. (Top) Cellular viability from the polymer screen. Viability given relative to untreated cells. (Bottom) Correlation between particle diameter and weight loss in mice at 24 hours for the partial factorial formulation screen. Dotted lines indicate 95% confidence interval for a liner regression model (*n* = 3).

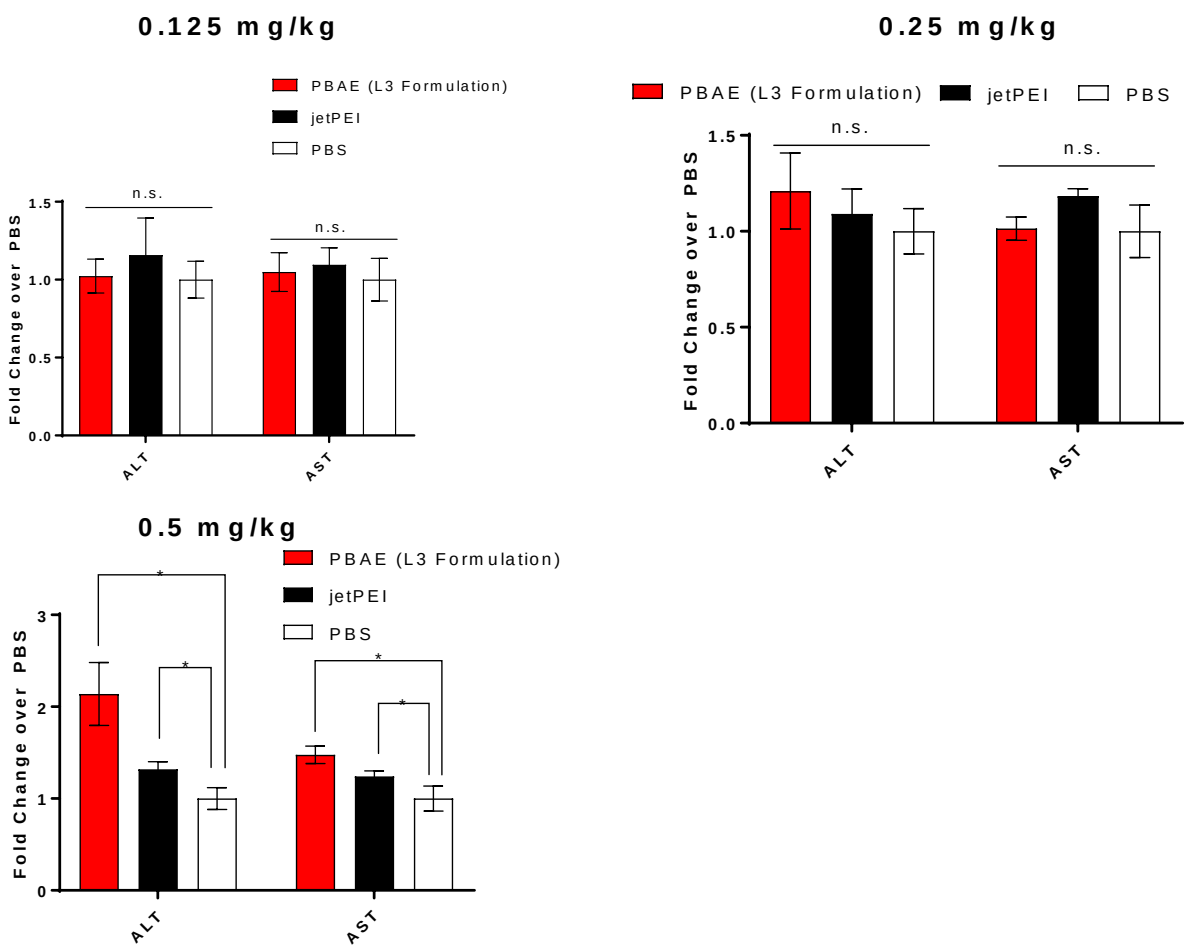

Figure S11. Liver enzyme levels (* indicates $p<0.05$) following optimized A1-L3 nanoparticle injection of various doses at 24 hours ($n = 3$).

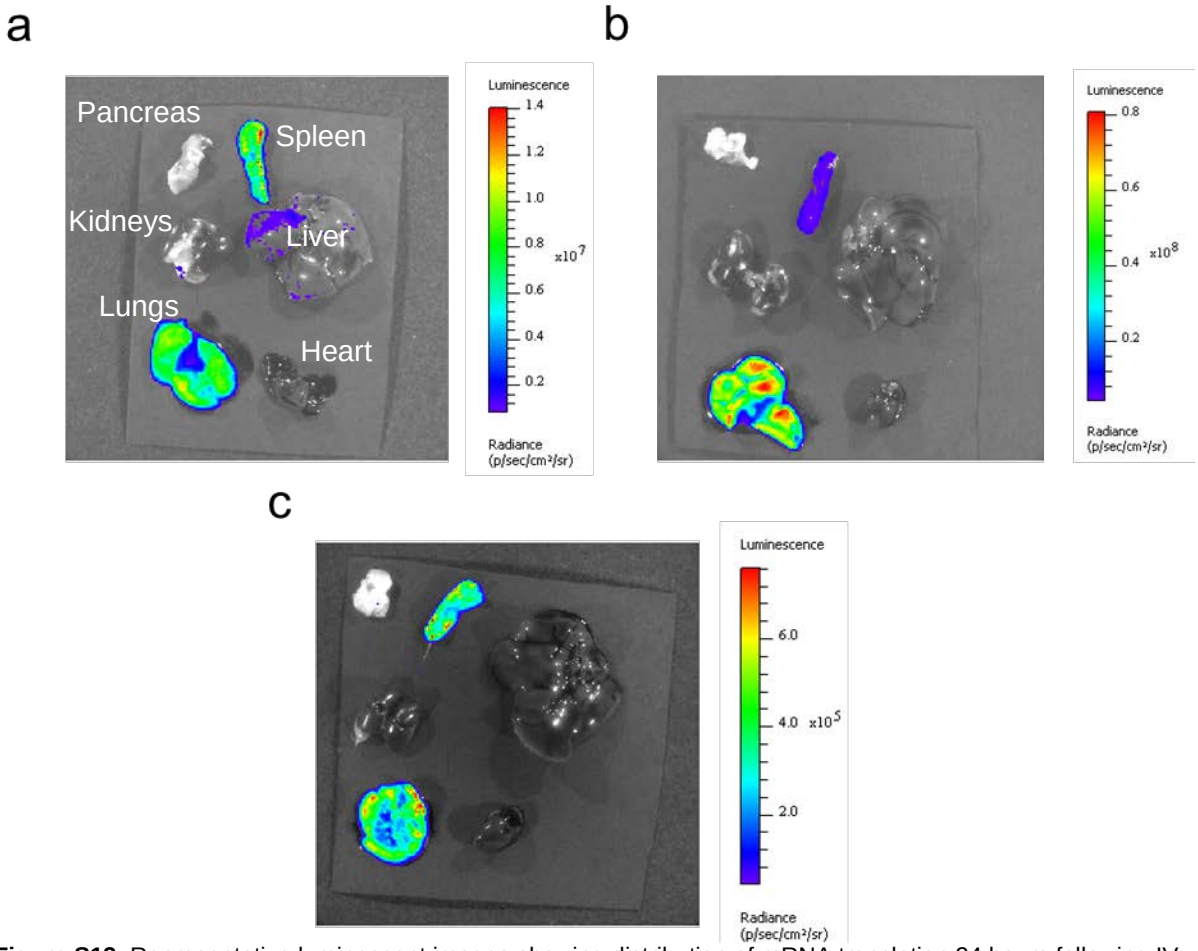

Figure S12. Representative luminescent images showing distribution of mRNA translation 24 hours following IV administration of control A1 particles formulated with 7 mol% C14-PEG2000 (a), optimized A1-L3 particles (b), and *in vivo* jetPEI (c). All particles administered at 0.5 mg/kg mRNA dose. Note differences in scale bars.

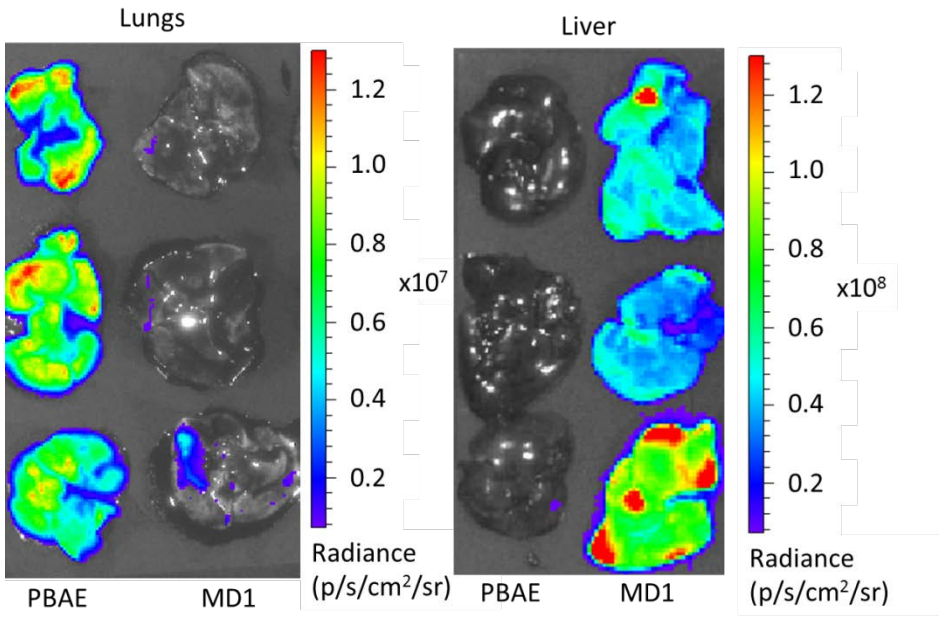

Figure S13. Comparison of luciferase mRNA delivery efficacy in both lungs and liver at 24 hours using optimized A1-L3 nanoparticles and a leading lipid nanoparticle, cKK-E12 (also known as MD1)[6] (0.5 mg/kg mRNA dose).

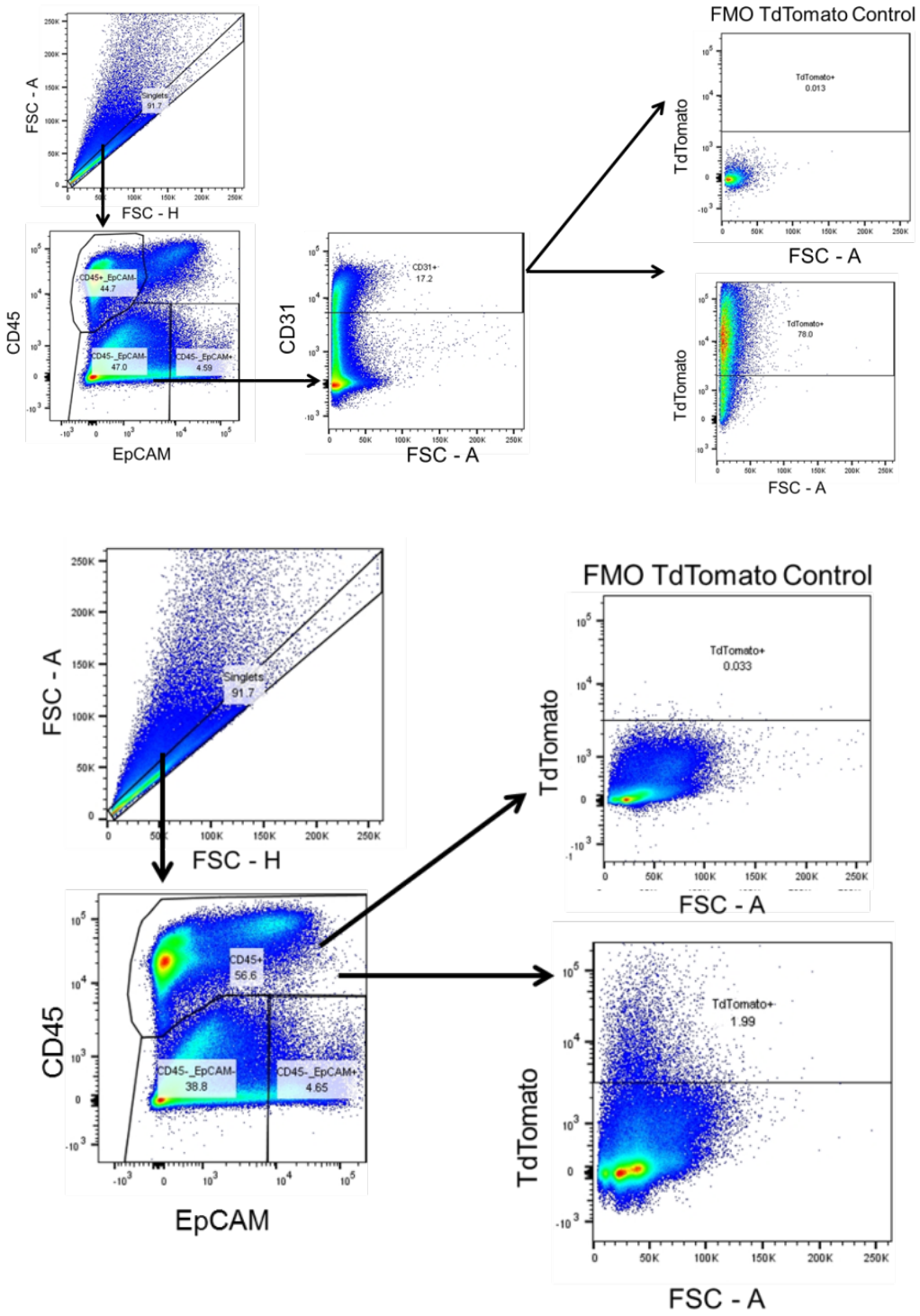

Figure S14. Gating strategy for identifying tdTomato positive endothelial (top) and immune (bottom) cells.

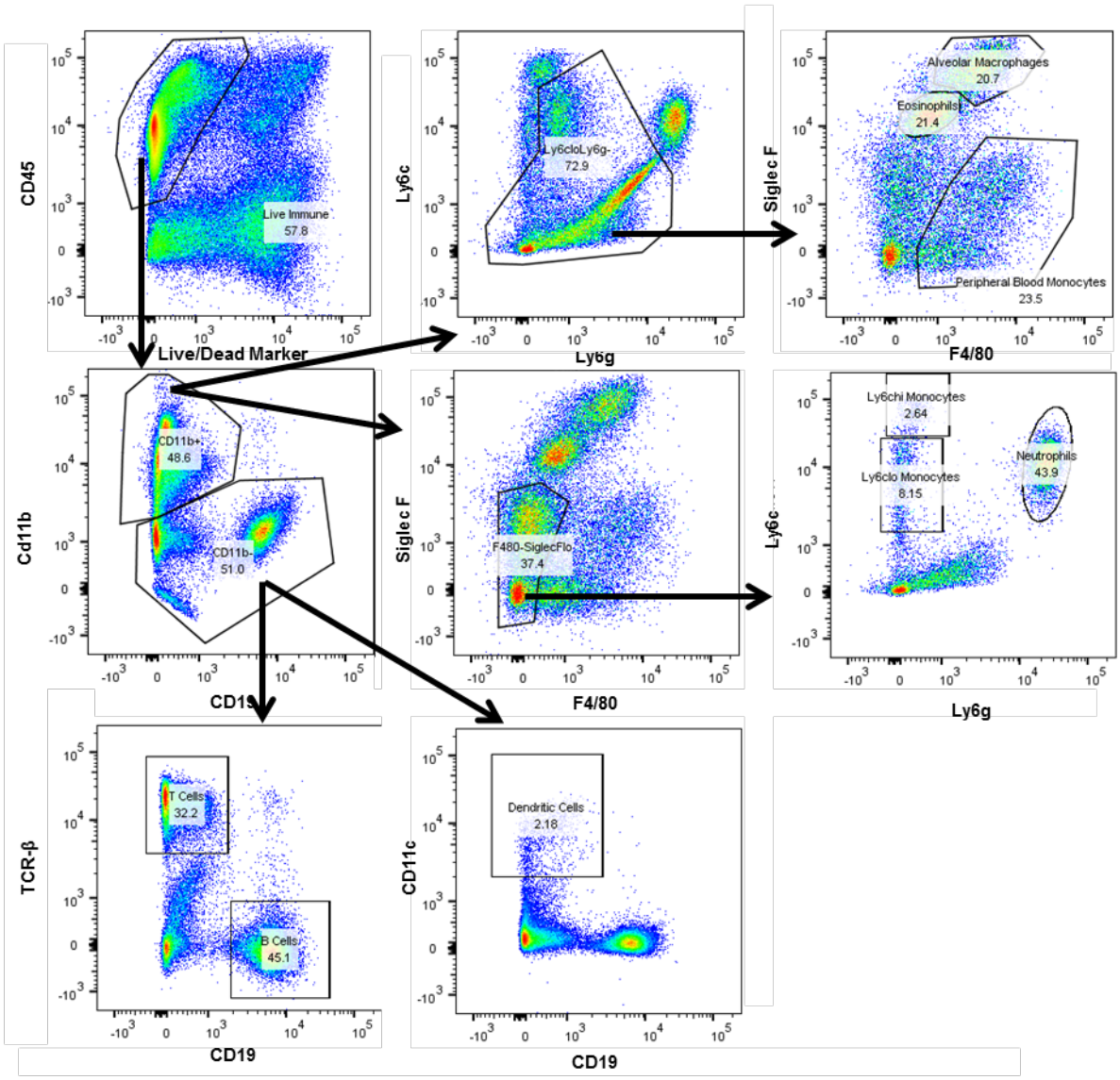

Figure S15. Gating strategy for identifying lung immune cell populations.

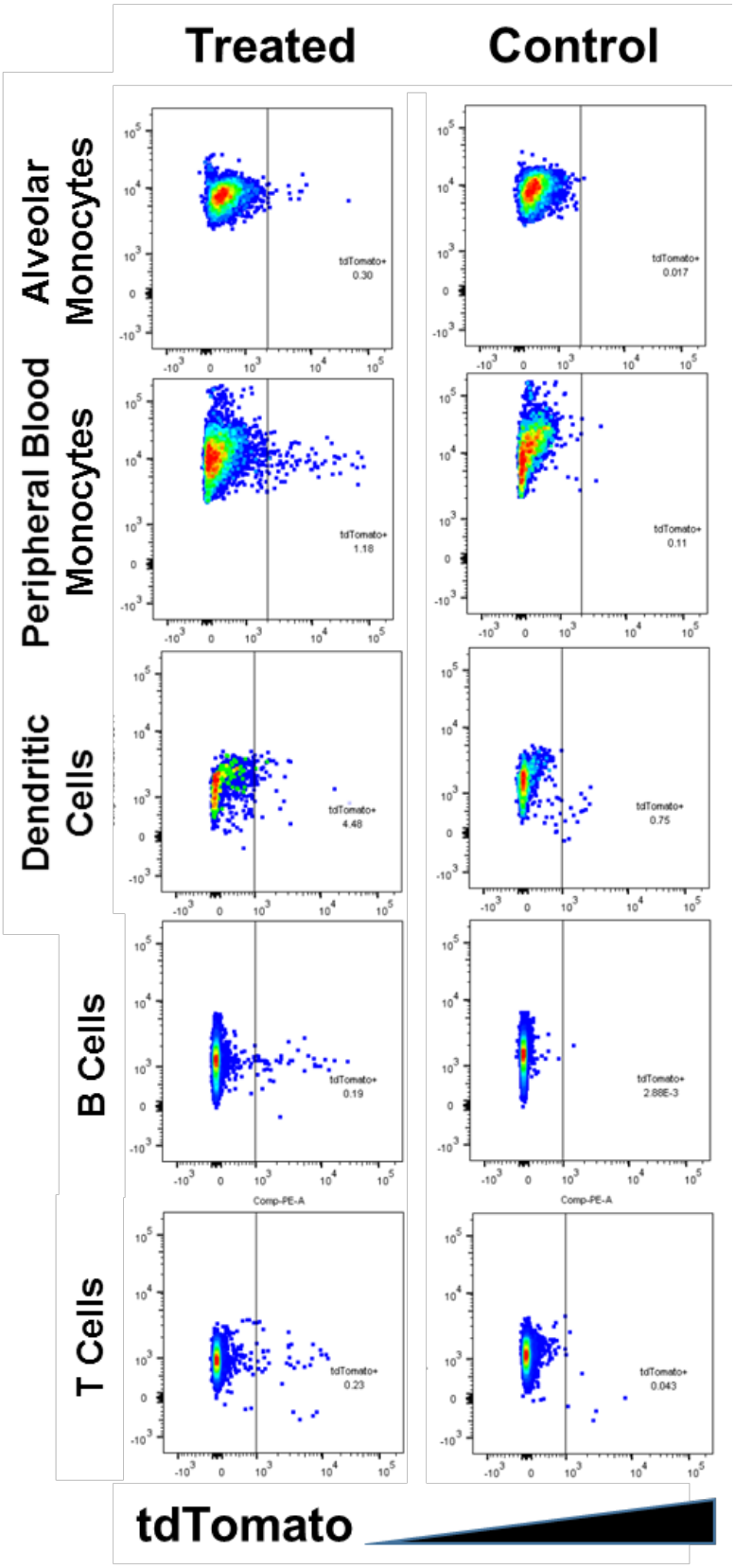

Figure S16. Gating for tdTomato positive immune cells (x axis).

Table S7: Antibodies used in FACS analysis

Antigen	Color	Dilution	Supplier	Clone
CD31	AF488	1:300	BioLegend	MEC13.3
CD45	BV421	1:300	BioLegend	104
CD45.2 (Immune Subtype Study)	BUV737	1:100	Becton Dickinson	104
TCR-β	BV421	1:200	BioLegend	H57-597
Ly6G	BV510	1:400	BioLegend	1A8
Siglec F	BV605	1:200	Becton Dickinson	E50-2440
Ly6C	AF488	1:400	Becton Dickinson	HK1.4
CD11c	PerCP/Cy5.5	1:250	BioLegend	N418
F4/80	PE/Cy7	1:250	BioLegend	BM8
CD19	APC	1:300	BioLegend	6D5
CD11b	AF700	1:400	BioLegend	M1/70

5. Works Cited

(1) Fulmer, G. R.; Miller, A. J. M.; Sherden, N. H.; Gottlieb, H. E.; Nudelman, A.; Stoltz, B. M.; Bercaw, J. E.; Goldberg, K. I. *Organometallics* **2010**, *29* (9), 2176–2179.

(2) Chen, D.; Love, K. T.; Chen, Y.; Eltoukhy, A. A.; Kastrup, C.; Sahay, G.; Jeon, A.; Dong, Y.; Whitehead, K. A.; Anderson, D. G. *J. Am. Chem. Soc.* **2012**, *134* (16), 6948–6951.

(3) Clark, J. B.; Dean, A. M. *Stat. Sin.* **2001**, *11* (2), 537–547.

(4) Kauffman, K. J.; Dorkin, J. R.; Yang, J. H.; Heartlein, M. W.; DeRosa, F.; Mir, F. F.; Fenton, O. S.; Anderson, D. G. *Nano Lett.* **2015**, *15* (11), 7300–7306.

(5) Kaczmarek, J. C.; Patel, A. K.; Kauffman, K. J.; Fenton, O. S.; Webber, M. J.; Heartlein, M. W.; DeRosa, F.; Anderson, D. G. *Angew. Chemie Int. Ed.* **2016**, *55* (44), 13808–13812.

(6) Dong, Y.; Love, K. T.; Dorkin, J. R.; Sirirungruang, S.; Zhang, Y.; Chen, D.; Bogorad, R. L.; Yin, H.; Vegas, A. J.; Alabi, C. A.; et al. *Proc. Natl. Acad. Sci.* **2014**, *111* (15), 5753–5753.